Synthesis and characterization of Polyvinylidiene Flouride–$Ba_{0.7}Sr_{0.3}TiO_3$ Nanocomposites

A dissertation submitted in the partial fulfillment of requirement for the award of the Degree of

Master of Science
in
Physics

Submitted by
Shobhneek kaur
Roll no.-301204010

Under the esteemed guidance of
Dr. Dwijendra P. Singh
(Assistant Professor)

School of Physics and Materials Science
Thapar University
Patiala (Punjab)-147004

July 2014.

DEDICATED TO MY PARENTS

CERTIFICATE

This is to certify that the thesis entitled **"Synthesis and Characterization of Polyvinylidieneflouride (PVDF)-$Ba_{0.7}Sr_{0.3}TiO_3$ Nanocomposite"** being submitted by **Shobhneek kaur (Roll No.301204010)** of M.Sc. (physics), Thapar University, Patiala. She has carried out by her under my supervision. She has not submitted this material for credits towards any other degree at Thapar University, Patiala or any other university.

Dr. Dwijendra P. Singh

Supervisor

(Assistant Professor),

School of Physic and Material Science,

Thapar University,

Patiala.

Dr. Kulvir Singh

Professor and Head

School of Physics and Material science

Thapar University,

Patiala

Dr. S. K, Mohapatra

Dean of Academic Affairs,

Thapar University,

Patiala

ACKNOWLEDGEMENT

I humbly prostrate myself before the Almighty for his grace and abundant blessings which enabled me to complete this work successfully.

It gives me immense pleasure to express my deep sense of gratitude to my supervisor **Dr. Dwijendra P. Singh,** School of physic and Material Science, Thapar University, Patiala for providing his invaluable guidance, motivation constant inspiration and above all his ever co-operating attitude enabled me in bringing up this thesis in present elegant form.

I am extremely thankful to **Dr. Kulvir Singh** (professor and head) Department of School of Physics and Materials Science and the faculty members of all Physics department for providing me all kinds of possible help and advice during the course of this work.

I would like to put my heartiest gratitude to my whole family for their constant support enthusiasm and encouragement.

In last but not the least I would like to thank my friends Ms. Pallavi Gupta, Paramjot Jha, Gaurav Singla and Tamanna Vilacha all those people who have helped me directly or indirectly to do my project work.

Shobhneek Kaur

Ms. Shobhneek kaur

Roll no: 301204010

Date:15 July, 2014

Place: Thapar University Patiala

DECLARATION

I hereby declare that the Dissertation **"Synthesis and Characterization of Polyvinylidieneflouride (PVDF)-$Ba_{0.7}Sr_{0.3}TiO_3$ Nanocomposite"** is the work carried out by me under the supervision of **Dr. Dwijendra P. Singh**. I have not submitted this work anywhere else for the award of any degree.

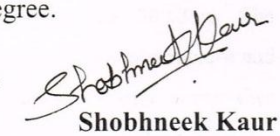

Shobhneek Kaur

ABSTRACT

The Lead free, Barium Strontium Titanate $Ba_{0.7}Sr_{0.3}TiO_3$ has been synthesized by Sol-Gel method. The synthesized sample has been subjected to the structural, morphological studies. The formation of the compound has been confirmed by X-Ray diffraction (XRD) analysis. The X-Ray Diffraction study confirmed that $Ba_{0.7}Sr_{0.3}TiO_3$ has tetragonal phase with crystalline size 30.53nm. The SEM studies have shown the good morphological structure and the average grain size of $Ba_{0.7}Sr_{0.3}TiO_3$ has been found to be 1.9 μm. The polymer ceramic composites have prepared using Polyvinylidene fluoride (PVDF) as polymer matrix and $Ba_{0.7}Sr_{0.3}TiO_3$ (BST) as ceramics powder by Solution Casting method. The surface morphology and thermal study of the BST/PVDF composites with different loading percentage have been done by the SEM and DSC.

TABLE OF CONTENTS

LIST OF FIGURES

LIST OF TABLES

CHAPTER: 1

Introduction

1.1 Introduction:

Ferroelectricity was discovered in 1921 by J. Valasek during an investigation of the anomalous dielectric properties of Rochelle salt ($NaKC_4H_4O_6 \cdot 4H_2O$). A second ferroelectric material, KH_2PO_4, was not found until 1935 and was followed by some of its isomorphs. The third major substance, $BaTiO_3$, was reported by A. Von Hippel in 1944, since then, this small group has been joined by [~250] pure materials and many more mixed crystal systems. Barium Strontium Titanate is a well-known ferroelectric material having a ferroelectric transition temperature that can be tuned by varying the Ba/Sr ratio. Barium strontium titanate (BST) is a solid solution of barium titanate and strontium titanate having high dielectric constant, low dielectric loss, low leakage current density and good thermal stability [1]. To improve the ferroelectric properties, $BaTiO_3$ was doped with some metals such as calcium, zirconium, tin and strontium. Strontium show good dielectric properties. Barium strontium titanate ($BaSrTiO_3$) powder is a high interest electronic material due to its high dielectric constant, alterable Curie temperature with composition, low dielectric loss, and high tunability of the dielectric behavior. $BaSrTiO_3$ has been widely used in the preparation of high dielectric capacitors, PTC resistors, transducers, piezoelectric sensors, dynamic random access memories, microwave phase shifters, and uncooled infrared detectors [2]. In this project, barium strontium titanate was fabricated and study at different concentration of barium and strontium.

1.2 (a) Ferroelectrics:

A group of dielectric materials that display spontaneous polarization. In other words, they possess polarization in the absence of an electric field. Ferroelectricity is a property of

certain materials that have a spontaneous electric polarization that can be reversed by the application of an external electric field. The term is used in analogy to ferromagnetism in which a material exhibits a permanent magnetic moment.

1.2 (b) Effect of temperature on ferroeleclectrics:

Ferroelectric materials tend to become paraelectric beyond a transition temperature called Curie temperature T_c. At the Curie temperature, the ferroelectric materials undergo a structural change from ferroelectric to paraelectric attaining highest dielectric constant. The transition characteristic of ferroelectrics is shown in Figure 1.1.

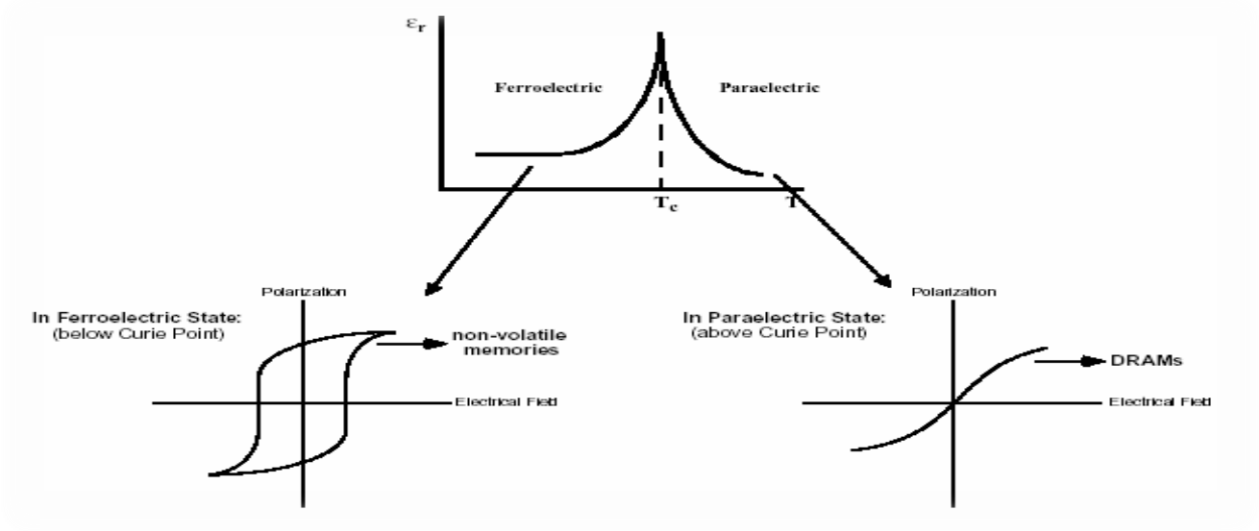

Figure 1.1 Transition characteristic of ferroelectrics

As shown in Figure 1.1, in the ferroelectric phase, the dielectric constant of the increases as the temperature increases. While in the Para electric phase, the dielectric constant decreases with increase in temperature obeying the Curie-Weiss. The Curie-Weiss law is given as follows:

$$\varepsilon_r = \frac{C}{T - Tc}$$

Where ε_r is the relative dielectric constant, T_c is the Curie temperature, T is temperature and C is a constant. ε_r attains its maximum value at T_c and for $T > T_c$, ε_r decreases sharply. In the ferroelectric phase, a strong hysteresis behavior is observed and it makes

the ferroelectric material suitable for nonvolatile memory applications. Above the Curie temperature, in the Para electric phase, the material no longer has spontaneous polarization. However the dielectric constant still remains high and hence the ferroelectric material is highly suitable for DRAM and tunable microwave applications [4, 5].

1.3 Dielectric Materials:

A dielectric material is a substance that is a poor conductor of electricity, but an efficient supporter of electrostatic field. If the flow of current between opposite electric charge poles is kept to a minimum while the electrostatic lines of flux are not impeded or interrupted, an electrostatic field can store energy. This property is useful in capacitors, especially at radio frequencies. Dielectric materials are also used in the construction of radio-frequency transmission lines. An important property of a dielectric is its ability to support an electrostatic field while dissipating minimal energy in the form of heat. The low the dielectric loss (the proportion of energy lost as heat), the more effective is a dielectric material [6].

1.4 Barium Strontium Titanate (BST):

BST ($Ba_xSr_{1-x}TiO_3$) is derived from the prototype $BaTiO_3$ (BTO) perovskite. In the case of normal ferroelectrics, BST undergoes phase transition at Curie temperature. However, Curie temperature depends on the Ba: Sr ratio. The isovalent additive, strontium (Sr^{+2}), has a high solid solubility and is the same valency as the replaced barium ion. The addition of strontium shifts the Curie temperature, for example, $Ba_{0.5}Sr_{0.5}TiO_3$ has a curie temperature of about -50°C and $Ba_{0.75}Sr_{0.25}TiO_3$ has a curie temperature of about +40°C. Interestingly, (Ba, Sr) TiO_3 solid solutions have higher dielectric constant at Curie temperature than pure BTO. BST is purely ferroelectrics and has spontaneous polarization below T_c. The tunability of BST is also very high in the ferroelectric phase especially near T_c. However the dielectric losses are also very high in this region and hence this phase of BST finds applications in non-volatile memories. Above T_c, BST becomes Paraelectric and the hysteresis effect is not predominant. This region serves well

for tunable microwave device applications due to the associated high dielectric constant losses [7].

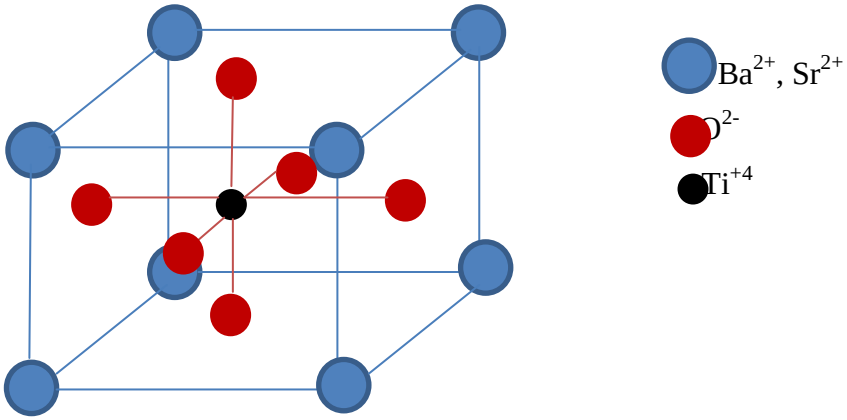

Figure 1.2 Structure of Barium Strontium Titanate

The phase transition with respect to temperature:

Temperature(^{o}C)	**Phase**	**Structure**
At 0^{o}C	Ferroelectric	Orthorhombic
0-90^{o}C	Ferroelectric	Rhombohedra
90-120^{o}C	Ferroelectric	Tetragonal
Above 120^{o}C	Paraelectric	Cubic

Table: 1

1.5 Modern classification of phase symmetry:

According to the Ehrenfest's original definition was that a first-order transition exhibit a discontinuity in the first derivative of the free energy with respect to some thermodynamic parameter, whereas a second-order transition has a discontinuity in the second derivative. Though useful, Ehrenfest's classification has been found to be an inaccurate method of classifying phase transitions, for it does not take into account the case where a derivative of free energy diverges (which is only possible in the thermodynamic limit).

According to modern phase transition are divided into two broad categories, named similarly to the Ehrenfest classes:

First-order phase transitions are those that involve a latent heat. During such a transition, a system either absorbs or releases a fixed amount of energy. During this process, the

temperature of the system will stay constant as heat is added: the system is in a "mixed-phase regime" in which some parts of the system have completed the transition and others have not.

Second-order phase transitions are also called continuous phase transitions. They are characterized by a divergent susceptibility, an infinite correlation length, and a power-law decay of correlations near criticality.

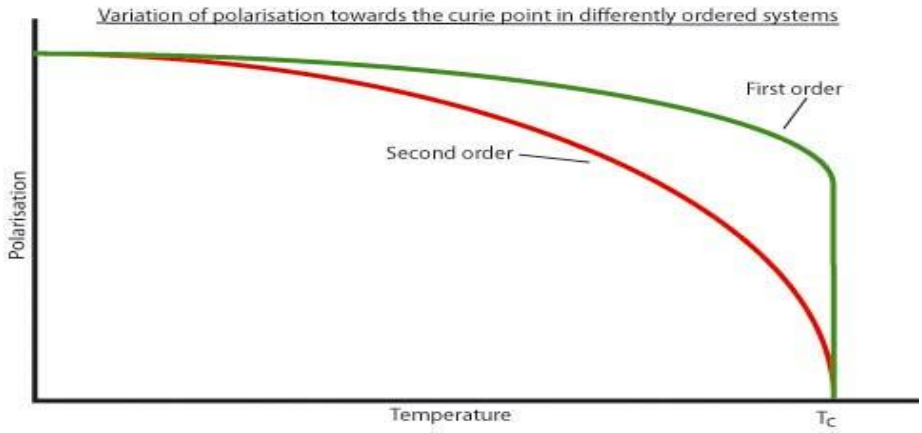

Fig 1.3 Graph of variation of polarization towards the curie point.

- In first order the polarization varies continuously until Curie temperature and after this there is discontinuity.
- In second order transition polarization varies continuously.

1.6 Ceramic Polymer composite:

Polymers are formed by chemical reactions in which a large number of molecules called monomers are joined sequentially, forming a chain. Polymers are substances whose molecules have high molar masses and are composed of a large number of repeating units. There are both naturally occurring and synthetic polymers. Synthetic polymers are produced commercially on a very large scale and have a wide range of properties and uses. The materials commonly called plastics are all synthetic polymers [8]. A composite material is made by combining two or more materials. They have different properties.

The two materials work together to give the composite unique properties. However, within the composite you can easily tell the different materials apart as they do not dissolve or blend into each other.

1.7 Nano composite:

- Nano composites are a class of materials in which one or more phases with Nano scale dimensions (0-D, 1-D, and 2-D) are embedded in a metal, ceramic, or polymer matrix.
- The general idea behind the addition of the Nano scale second phase is to create a synergy between the various constituents, such that novel properties capable of meeting or exceeding design expectations can be achieved
- The properties of nanocomposites rely on a range of variables, particularly the matrix material, which can exhibit nanoscale dimensions, loading, degree of dispersion, size, shape, and orientation of the nanoscale second phase and interactions between the matrix and the second phase [9].

.

CHAPTER 2

Experimental Details

2.1 Characterization Techniques:

Characterization techniques are used simply to magnify the specimen, to visualize its internal structure, and to gain knowledge as to the distribution of elements within the specimen and their interactions. These techniques include X-Ray Diffraction, Scanning Electron Microscope (SEM), Differential Scanning Calorimeter (DSC), Dielectric measurements.

2.1.1 X- Ray Diffraction (XRD):

Diffraction of light means the bending of light round the corners of an obstacle. X-rays, like other electromagnetic rays can also be diffracted. But for the diffraction of X-rays, the size of obstacle should be few angstroms which are approximately the wavelength of X-rays. X-rays were discovered by Roentgen, he called them X-rays because their nature at first was unknown so, and X-rays were also called Roentgen rays. The X-rays lie in the range of $0.1\ \text{Å} < \lambda < 1000\ \text{Å}$.

Phenomenon of X-Ray Diffraction:

When the mono chromatic X-rays are incident on a crystal, the atomic electrons in the crystal are set into vibrations with the same frequency as that of the frequency of the incident rays and are accelerated. These accelerated electrons then emit the radiations of the same frequency as that of incident X-rays in all the directions. If the wavelength of the incident radiations is large compared to the dimensions of the crystal, then the radiated X-rays are in the phase with each other. But since the atomic dimensions are nearly equal to the wavelength of X-rays, the radiations emitted by the electrons are out

of phase with each other. These radiations may interfere constructively or destructively, producing a diffraction pattern in certain directions.

2.1.2 Bragg's Law of Diffraction:

A regular array of scatters produces a regular array of spherical waves. Although these waves cancel one another out in most directions through destructive interference, they add constructively in a few specific directions, determined by Bragg's law:

$$n\lambda = 2d\sin\theta$$

Here d is the spacing between diffracting planes, theta is the incident angle, n is any integer, and λ is the wavelength of the beam. These specific directions appear as spots on the diffraction pattern called reflections. Thus, X-ray diffraction results from an electromagnetic wave (the X-ray) impinging on a regular array of scatters (the repeating arrangement of atoms within the crystal). X-rays are used to produce the diffraction pattern because their wavelength λ is typically the same order of magnitude (1–100 angstroms) as the spacing d between planes in the crystal.

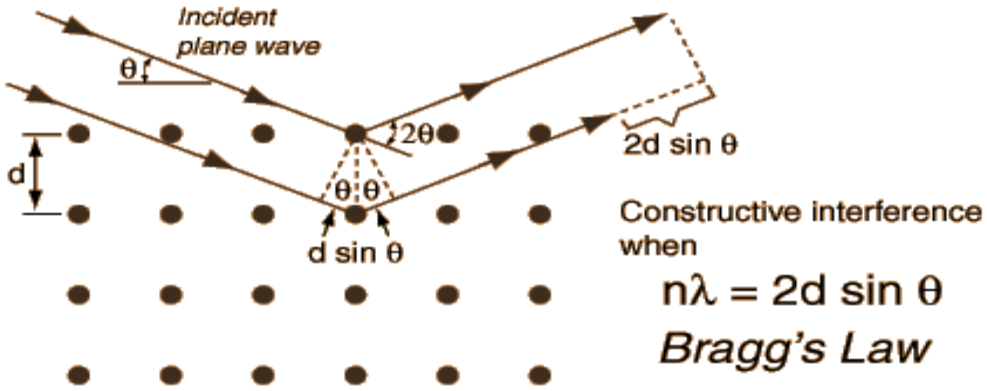

Figure 2.1 Bragg's law

Diffraction peak positions are accurately measured with XRD, which makes it the best method for characterizing homogeneous and inhomogeneous strains. In homogeneous strains vary from crystallite to crystallite or within a single crystallite and this causes a broadening of the diffraction peaks that increases with the sine of angle (θ) [10].

Figure 2.2 X-Ray Diffraction

2.1.3 Scanning Electron Microscope (SEM):

SEM stands for scanning electron microscope. The SEM is a microscope that uses electrons instead of light to form an image. The SEM has a large depth of field, which allows more of a specimen to be in focus at one time. The SEM also has much higher resolution, so closely spaced specimens can be magnified at much higher levels. Because the SEM uses electromagnets rather than lenses, the researcher has much more control in the degree of magnification.

The SEM is an instrument that produces a largely magnified image by using electrons instead of light to form an image. A beam of electrons is produced at the top of the microscope by an electron gun. The electron beam follows a vertical path through the microscope, which is held within a vacuum. The beam travels through electromagnetic fields and lenses, which focus the beam down toward the sample. Once the beam hits the sample, electrons and X-rays are ejected from the sample.

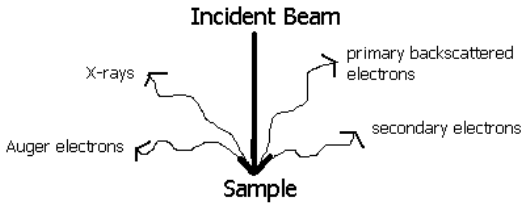

Fig: 2.3 Incident beam on the Sample

Detectors collect these X-rays, backscattered electrons, and secondary electrons and convert them into a signal that is sent to a screen similar to a television screen. This produces the final image.

Figure 2.4 Apparatus of Scanning Electron Microscope

2.1.4 Electron dispersive X-ray spectroscopy (EDXS) Analysis:

When the sample is bombarded by the SEM's electron beam, electrons are ejected from the atoms comprising the sample's surface. The resulting electron vacancies are filled by electrons from a higher state, and an X-ray is emitted to balance the energy difference between the two electrons' states. The X-ray energy is characteristic of the element from which it was emitted.

The EDS X-ray detector measures the relative abundance of emitted X-rays versus their energy. The detector is typically lithium-drifted silicon, solid-state device. When an incident X-ray strikes the detector, it creates a charge pulse that is proportional to the energy of the X-ray. The charge pulse is converted to a voltage pulse by a charge-sensitive preamplifier. The signal is then sent to a multichannel analyzer where the pulses are sorted by voltage. The energy, as determined from the voltage measurement, for each incident X-ray is sent to a computer for display and further data evaluation. The spectrum

of X-ray energy versus counts is evaluated to determine the elemental composition of the sampled volume.

2.1.5 Differential Scanning Calorimeter (DSC):

The term DSC was coined to describe this instrument which measures energy directly and allows precise measurements of heat capacity. Differential Scanning Calorimeter or DSC is a thermo analytical technique in which the difference in the amount of heat required to increase the temperature of a sample and reference is measured as a function of temperature. Both the sample and reference are maintained at nearly the same temperature throughout the experiment. Generally, the temperature program for a DSC analysis is designed such that the sample holder temperature increases linearly as a function of time. The reference sample should have a well-defined heat capacity over the range of temperatures to be scanned.

DSC is used widely for examining polymeric materials to determine their thermal transitions. The observed thermal transitions can be utilized to compare materials, however, the transitions do not uniquely identify composition. Melting points and glass transition temperatures for most polymers are available from standard compilations, and the method can show polymer-degradation by the lowering of the expected melting point, T_m, for example. T_m depends on the molecular weight of the polymer and thermal history, so lower grades may have lower melting points than expected. The percent crystalline content of a polymer can be estimated from the crystallization/melting peaks of the DSC graph.

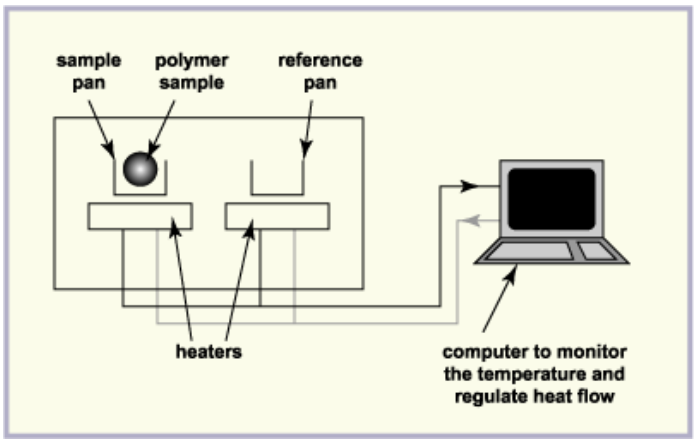

Fig: 2.5 Instrument of DSC

2.2 Powder Synthesis:

Sol Gel Method:

To prepare a Barium strontium titanate in powder we use a sol gel method. The sol-gel process may be described as: "Formation of an oxide network through polycondensation reactions of a molecular precursor in a liquid." A sol is a stable dispersion of colloidal particles or polymers in a solvent. The particles may be amorphous or crystalline. An aerosol is particles in a gas phase, while a sol is particles in a liquid. A gel consists of a three dimensional continuous network, which encloses a liquid phase, in a colloidal gel, the network is built from agglomeration of colloidal particles. In a polymer gel the particles have a polymeric sub-structure made by aggregates of sub-colloidal particles. Generally, the sol particles may interact by van der Waals forces or hydrogen bonds. A gel may also be formed from linking polymer chains. In most gel systems used for materials synthesis, the interactions are of a covalent nature and the gel process is irreversible. The gelation process may be reversible if other interactions are involved.

Advantages:

- The idea behind sol-gel synthesis is to dissolve the compound in a liquid in order to bring it back as a solid in controlled manner.

- Multi component compounds may be prepared with a controlled stoichiometry by mixing sols of different compounds.
- The sol-gel method prevents the problems with co-precipitation, which may be inhomogeneous, be a gelation reaction.
- Enables mixing at an atomic level.
- Results in small particles, which are easily sinterable.

Synthesis by sol gel method:

Sol-gel synthesis may be used to prepare materials with a variety of shapes, such as porous structures, thin fibers, dense powders and thin films. If the gel is dried by evaporation, then the capillary forces will result in shrinkage, the gel network will collapse, and a xerogel is formed. If drying is performed under supercritical conditions, the network structure may be retained and a gel with large pores may be formed. This is called an aerogel, and the density will be very low. A record is < 0.005 g/cm^3. After the making of an aerogel we calcined it. Calcination is a process of heating a substance to a high temperature but below the melting or fusing point, causing loss of moisture, reduction or oxidation, and dissociation into simpler substances. We calcine it at 900^{0}C [11].

Preparation of $Ba_{0.7}Sr_{0.3}TiO_3$ by Sol-gel method:

The process can be explained as follows:

- Solution I is prepared by mixing of barium acetate with acetic acid by stirring and heating it for 40 min at70^0 C.
- Solution II is prepared by mixing of strontium acetate with acetic acid by stirring and heating it for 40 min at 70^{0}C.
- Now add the solution I and II stir and heat it for 30 min at 70^{0}C. Let it consider as solution III.
- Solution IV is prepared by mixing of Titanium (IV) isopropoxide and 2-methoxyethanol by stirring and heating for 40 min at 70^{0}C.

- Now add the solution (III) and (IV) stir and heat it for 40 min at70^0c. Let it consider as solution (V).
- Add the acetic acid in solution (V) stir and heat it for 20 min at 70^0C.
- Take the solution (V) remain it for 24 hours without stirring and heating.
- After 24 hours heat and stir the solution (V) at 70^0C until the gel is form.
- Heating process is occurring till the gel form changes into crystal form.
- Grinding the crystal to form powder.
- Calcine that powder for 14 hours at 900^0 C [11].

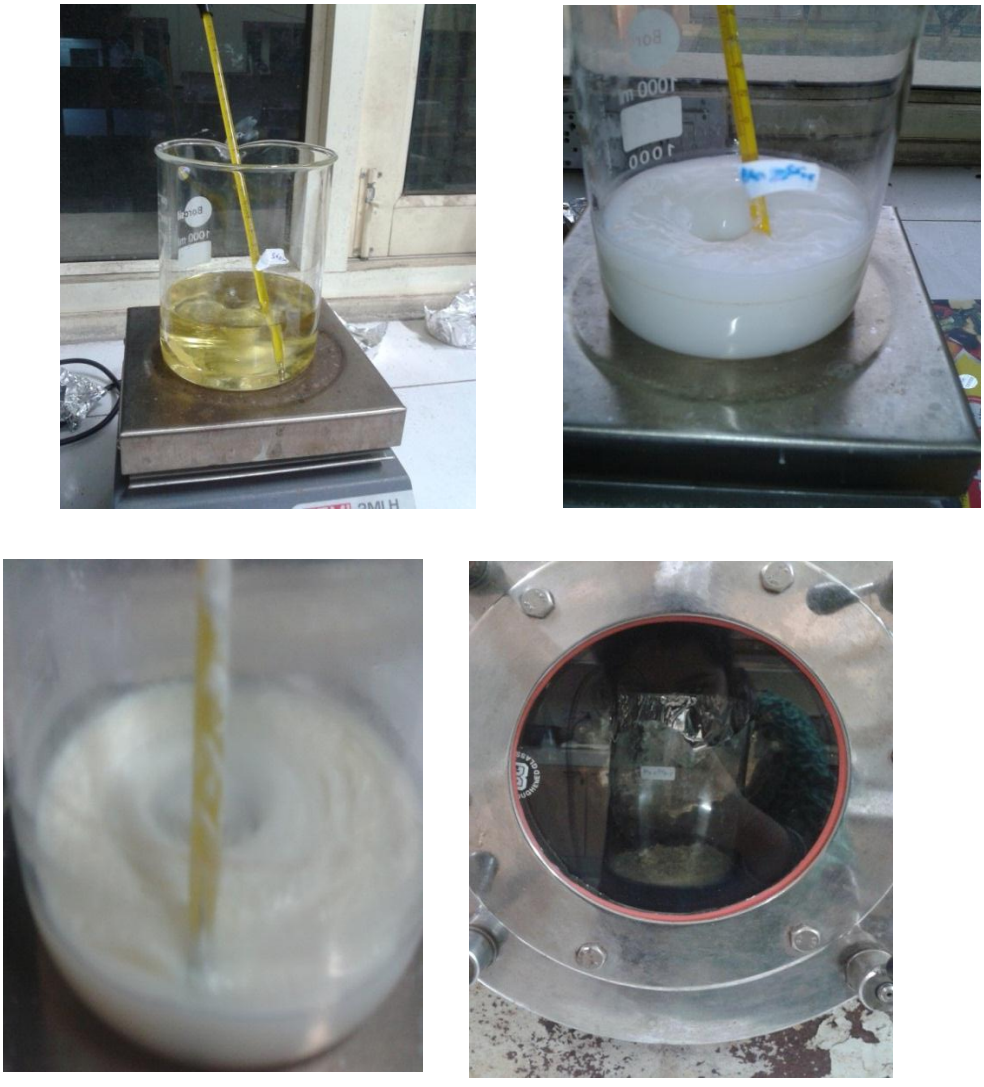

Figure 2.6 Schematic representation of sol-gel process for synthesis of nanoparticle.

2.2.1 Synthesis of $Ba_{0.7}Sr_{0.3}TiO_3$ Polymer Composite:

Materials are mainly classified into four main categories i.e. metals, plastics, ceramics and composites. Composites are generally artificial or naturally occurring materials that are made from the combination of two or more constituents having different physical and chemical properties. The composite materials are heterogeneous in nature.

Polymer ceramic composite is a combination of polymer and other ceramic material:

Polymer + ceramic = Polymer composite

Polymer has some merits like good mechanical property, easy to synthesize and high dielectric breakdown strength and having low dielectric constant [12].

To prepare a BST Nanocomposite having with polymer there are different methods like: Dip Coating method, Hot Pressing method, Tufting method and Solution Casting method. This work we use Solution Casting method.

2.2.2 Solution Casting Method:

Solution casting method is the one of the simplest and easiest method to prepare polymer composite. In this we mix the polymer in solvent according to weight percent ratio. Thus method is low cost method and therefore there is no need of any costly equipment's.

2.2.3 Preparation of $Ba_{0.7}Sr_{0.3}TiO_3$ Nano Composite by solution casting method:

- Mix 40 ml of Dimethylformamide (DMF) with Polyvinylidene fluoride (PVDF).
- Stir it and heat it at 70^0C for 2 hours.
- After that add $BaSrTiO_3$ in it and again stir and heat it at 70^0C until the solution gets thicker.
- After that pour the solution in petri-dish and remain it for 2-3 hours.

- Now put the petri-dish on heat at 70^0C and heat it until the film forms.

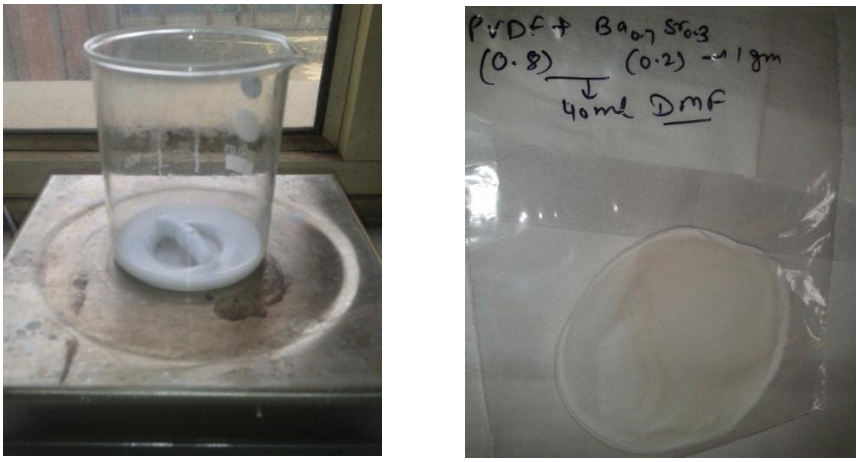

Figure 2.7 Composite of Barium Strontium Titanate

2.3 LITERATURE REVIEW:

1. Maensiri *et al.,* [1] it conclude that BST nanofibres are based on nanoparticle network, they should have both the electronic and mechanical properties different from micrometer-size grains and micrometer size fiber's. Nanofibres of BST have been successfully fabricated using and electro spinning and sol-gel techniques

2. Lahiry *et al.,* [6] synthesized $Ba_{0.4}Sr_{0.6}TiO_3$ dielectric properties by making it with sol-gel process mixing with ethanol. The dielectric loss is high at lower frequencies. The dielectric data is dependent on thickness which explained by barrier layer model.

3. Somani *et al.,* [7] synthesized and characterization of Nano crystalline of Barium Strontium Titanate powder by sol-gel processing. In this we can conclude that it is difficult to maintain the phase purity of Nano $Ba_{0.7}Sr_{0.3}TiO_3$ at elevated temperature.

4. Ivankovic *et al.,* [8] concludes that organic-inorganic hybrids became a great interest of new research. New organic –inorganic hybrids based on poly (methyl methacrylate) and silsesquioxane structures were prepared by in situ bulk polymerization. Silsequioxane structure formed as a result of glymo hydrolysis and condensation in the sol-gel process influence the glass transition temperature of PMMA

5. Li *et al.,* [9] according the electrical measurement the real part of permittivity of PVDF/$BaTiO_3$ Nano composite increase with increase in $BaTiO_3$ content. The electrical behavior of Nano graphite doped PVDF/BaTiO3 composites can be well interpreted using the percolation theory.

6**.** Verma *et al.,* [10] synthesized Nano crystalline of BST 70/30 powder of average size 18nm via sol-route. The dielectric constant decrease with increase in frequency upto 10 kHz, beyond it is constant. In it ac conductivity is a thermally activated process and the activation energy as calculated is 0.35eV.

7. Chanmal *et al.,* [11] showed that the nanoparticles are well dispersed in the PVDF matrix as evidenced by the scanning electron micrographs. It concludes that the dielectric permittivity increases with increase in $BaTiO_3$ content.

8. Hu *et al.,* [15] conclude that a paraelectric ceramic, $Ba_{0.7}Sr_{0.3}TiO_3$doped with 5 mol% Bi_2O_3 (BSBT) is chosen as the filler, where the Paraelectrics decrease the remanent polarization of the ferroelectric polymer matrix and Bi_2O_3 is used to increase the electrical displacement. BSBT fibers have been prepared via electro spinning and were modified with the surfactant dopamine. A dopamine interfacial layer coating on the fibers facilitates the homogeneous dispersion of the Nano fiber fillers in the P (VDF-TrFE) polymer matrix.

9. Barber et al., [16] conclude that dielectric materials in the form of polymer composite and Nanocomposite can be used for energy storage and pulse power applications. For good power application we need high breakdown field strength and high dielectric constant.

10. Stemme *et al.,* [17] it conclude the effect of thermal processing and iron doping in co-sputtered barium strontium titanate thin films that it have a partial tetragonal distorted crystal structure. Iron acceptor doping lead to enhancement of the material quality factor Q and with the increase in Q factor there is decrease in permittivity and tenability of the material.

11. Schumacher *et al.,* [18] investigate that the permittivity of $BaTiO_3$ filled polymer ceramic composite is dependent on different temperature range. This effect mainly caused by changes in a dominant lattice structure of the powder of $BaTiO_3$

12. Ben-Hui Fan *et al.,* [19] it conclude that the dielectric permittivity of tetragonal BT is more than 1200 and with Ferroelectricity at room temperature where cubic BT is much lower and without ferroelectricity. At low frequency, the dielectric permittivity of Nano composite film with small size BT nanoparticles shows significant increase.

13. Beier *et al.,* [20] conclude that Nano crystals of BST have been emerged into a PMDA-BAPB polyimide system to understand the effects of loading small perovskite fillers on the dielectric properties of the Nano composite. Polyimides are being explored as an alternative polymer component for Nano composites because of high thermal and chemical stability, low dielectric loss, and comparably high breakdown strength.

14. Gross *et al.,* [21] conclude that PMMA shows goods thermal stability, optical clarity and excellent weather and chemical resistance. The PMMA based composites and hybrids shown as an interesting material for development of electroluminescent devices and dielectric films for microelectronic applications.

15. A. W. M. de Laat *et al.,* [22] it concludes the colloidal stabilization of $BaTiO_3$ poly (vinyl alcohol) and water. In this the carboxylic acid groups *can* prevent the PVA from adsorption on the particle surface. $BaTiO_3$ dispersion is stabilizing by block copolymer of PVA and carboxylic group.

CHAPTER 3

Results and Discussion

The structural, morphological and elemental analysis of ceramic is carried out by using XRD, SEM, EDS and DSC respectively. The thermal study of nanocomposite has also been done. The results of these experimental investigations are discussed in the subsequent subsection.

3.1 XRD Analysis:

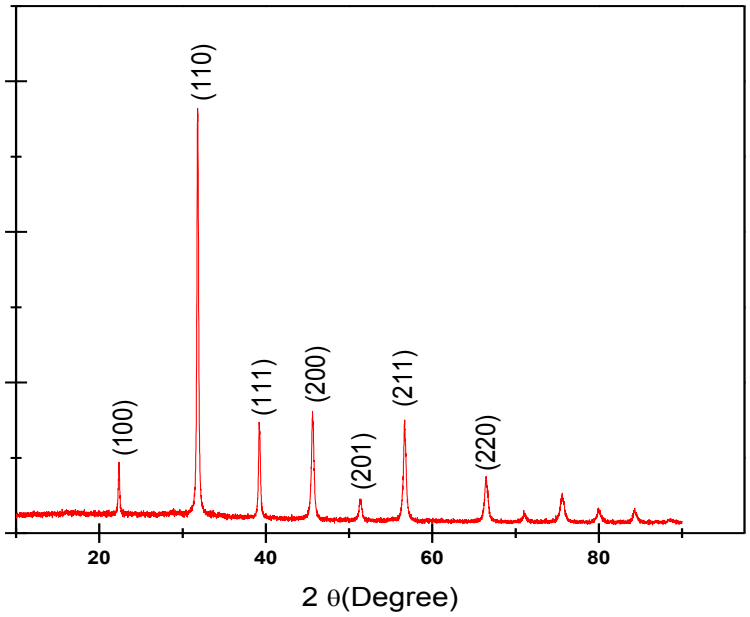

Figure 3.1 XRD pattern of Barium Strontium Titanate

The $Ba_{0.7}Sr_{0.3}TiO_3$ (BST) powder was derived as amorphous but transform to crystalline after calcination at 900^0C for 14 hours. Fig: 3.1 show the XRD analysis of nanoparticle where all the peaks are indexed and well matched to the tetragonal structure. The lattice parameter of calcined BST obtained from XRD analysis are a = b = 3.9724A^0, c =

3.9703A^0 (file No.$Ba_{0.7}$ xrdml). The crystalline size of $Ba_{0.7}Sr_{0.3}TiO_3$ was found using Scherer's formula to be 30.53nm. The crystalline size of BST nanoparticle can be calculated by Scherrer's formula.

$$d = \frac{k\lambda}{\beta cos\theta}$$

Where k is the shape factor (k=0.94), λ is the x-ray wavelength, β is the line broadening at half the maximum intensity (FWHM) in radians, and θ is the Bragg's angle, d is the crystallite size.[13]

3.2 SEM Analysis:

SEM micrograph of $Ba_{0.7}Sr_{0.3}TiO_3$ is shown in the fig.3.2. The average grain size of $Ba_{0.7}Sr_{0.3}TiO_3$ was to be found to be found to be 1.9 micrometer. This is actually not the size of BST nanoparticle; but this showing cluster of nanoparticles. The images of $Ba_{0.7}Sr_{0.3}TiO_3$ at magnification 1500x is shown in figure 3.2.

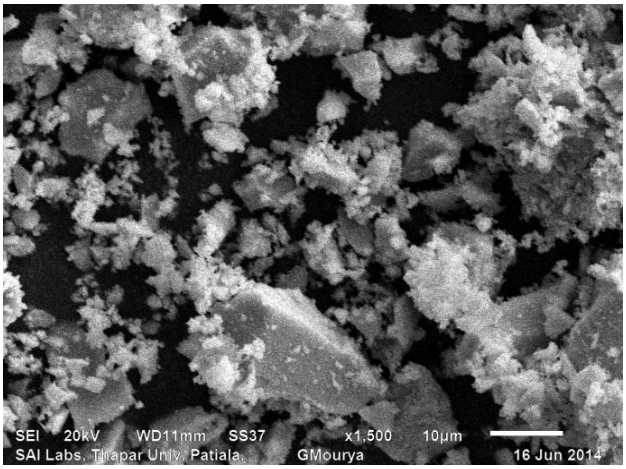

Fig 3.2 Scanning Electron Microscope of Barium Strontium Titanate 1500x.

3.3 Electron dispersive X-ray spectroscopy (EDXS) Analysis:

To find the elements present in the sample fabricated, EDXS (Energy-dispersive X-ray spectroscopy) was performed on the samples along with SEM analysis.

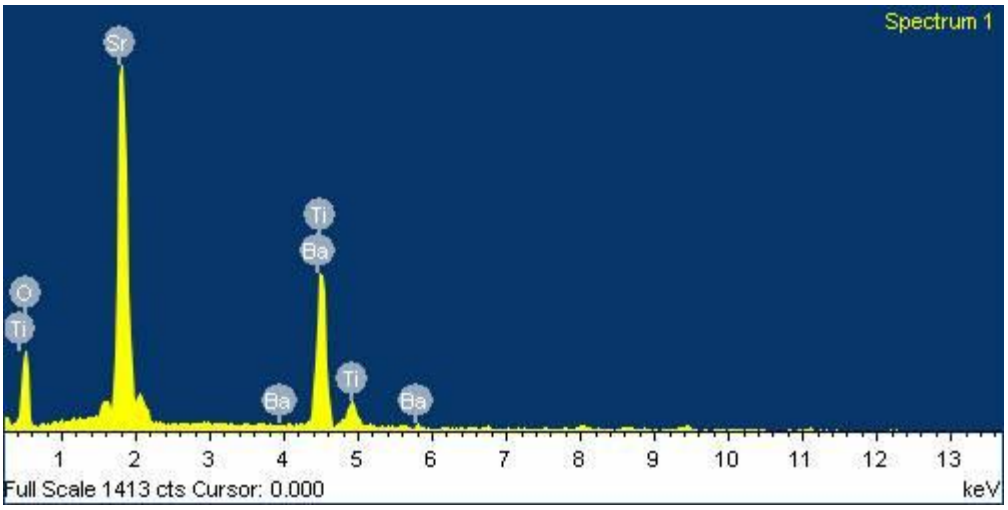

Figure 3.3 EDXS of $Ba_{0.7}Sr_{0.3}TiO_3$

The stoichiometric composition of titanium and oxygen is very close to 1:3 for the entire sample.

Element	**Atomic percent**
Oxygen	63.24
Titanium	15.27
Strontium	6.77
Barium	14.73

Table: 2

In synthesis of composition $Ba_{0.7}Sr_{0.3}TiO_3$ the ratio of Titanium and Oxygen comes out to be in given table.

Composition	Ratio of (Ba+Sr)/Ti	Ratio of (Ba+Sr)/O
$Ba_{0.7}Sr_{0.3}TiO_3$	1.40	2.99

Table: 3

According to the ratio of titanium and oxygen in this data comes out to be approximately close to 1:3. Therefore, $Ba_{0.7}Sr_{0.3}TiO_3$ is stiochiometrically correct.

3.4 SEM of BST Polymer Nano composite:

The SEM morphology of prepared powder is presented in figure: 3.4. It can be seen that nanoparticles are embedded in the PVDF matrix as the loading percent of BST up increasing in PVDF matrix then the connectivity of particle with matrix is decreases. Properly dispersed Nanoparticle in PVDF matrix has been synthesized and confirm from the SEM analysis. The lighter region in SEM show ferroelectric ceramic and darker region show polymer matrix.

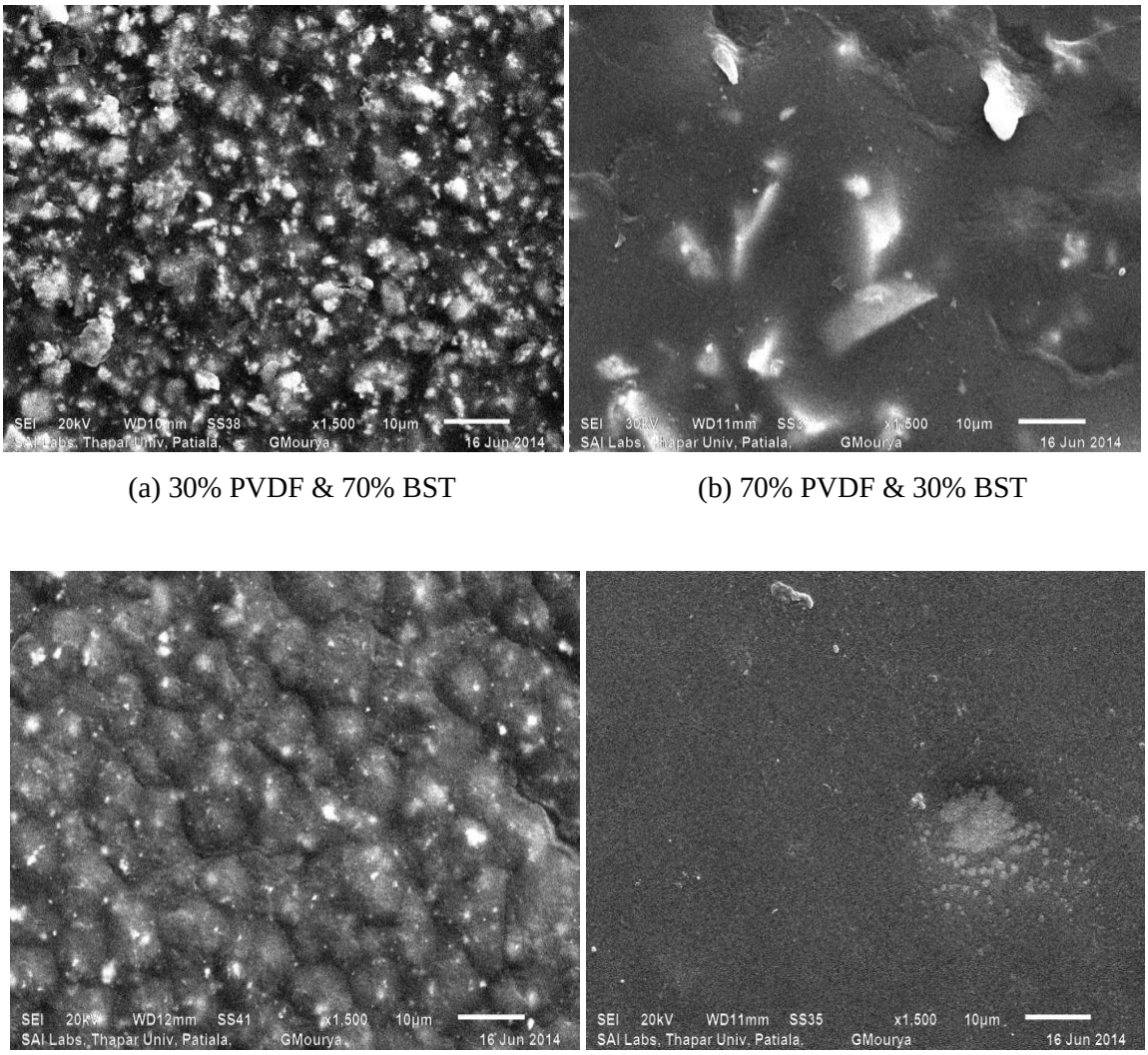

(a) 30% PVDF & 70% BST (b) 70% PVDF & 30% BST

(c) 50% PVDF & 50% BST (d) 100% PVDF

Figure 3.4 SEM micrograph of (a), (b) & (c) at different composition of PVDF and BST and (d) Pure PVDF

3.5 Differential Scanning Calorimetry curve of PVDF and $Ba_{0.7}Sr_{0.3}TiO_3$ NanoComposite:

The heating effects on the BST/PVDF composites are shown in figure 3.5. It can be seen that the filler has remarkable effect on the melting behavior of the composites. The composite samples were fractured in liquid argon before SEM observation. Differential Scanning Calorimetry (DSC) measurements were performed using a Shimadzu instrument DSC-60 in an argon atmosphere. The specimens were heated at 10^0C/min from 30^0C to 250^0C. The degree of crystallinity was measured by the ratio of the measured fusion heat, ΔH to that of a 100 percent crystalline PVDF, ΔH^0 and its value is 104.6 x 10^3 J/kg. Crystallinity has been calculated by the formula: [14]

$$X= \Delta H/\Delta H^0$$

Composition	Crystallinity (x)	Heat of fusion (ΔH)*10^3J/kg
73 PVDF- BST	0.499287	52.2753
55 PVDF-BST	0.537163	56.2409
37 PVDF-BST	0.482967	50.4964

Table: 4

The increase in weight percentage of crystallinity is found to be increase upto certain percentage of weight percentage of BST nanoparticle and; when weight percent of PVDF and BST 5:5 value of crystallinity of PVDF is found to be decreases. This point of transition is the perculation threshold of BST nanoparticle in PVDF Matrix.

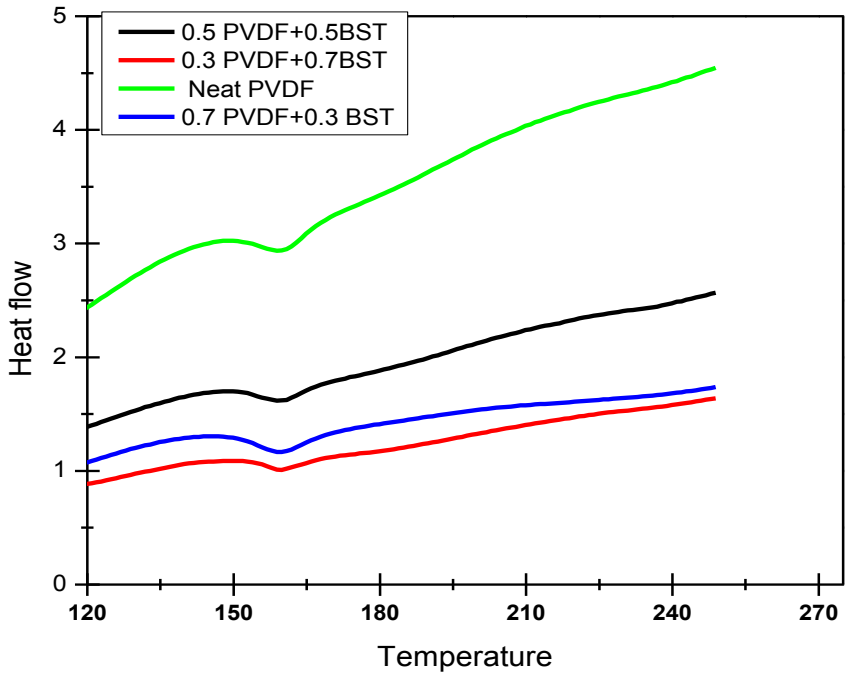

Figure 3.5Heat flow vs Temperature curve for PVDF- BST nanocomposite as recorded by DSC.

CHAPTER: 4

Conclusions and future scope

The conclusions of characterization and synthesis are follows:

4.1 Conclusion:

i. The sample of BST with stoichiometric Composition (Ba0.7Sr0.TiO3) has been successfully synthesized by Sol-Gel Technique.

ii. The results of XRD analysis have confirmed the phase formation or BST sample. The phase of $Ba_{0.7}Sr_{0.3}TiO_3$ was found to be tetragonal and cell parameters were found to be a = b = 3.979087 and c = 3.97093A^0 and crystalline size is come out to be 30.53 nm.

iii. The SEM of sintered sample has shown good surface morphology and average grain size of $Ba_{0.7}Sr_{0.3}TiO_3$ was found to be 1.9 micrometer.

iv. The EDS studies of BST show the stoichiometric ratio is comes out to be approximately 1:3.

v. The BST/PVDF Composite has been synthesized by Solution Casting Method.

vi. The SEM studies shows nanoparticles are embedded in the PVDF matrix. Connectivity decreases with increase in weight percent of BST in PVDF.

vii. The DSC studies shows change in Heat flow with change in temperature. Crystallinity first increase and then decreases with weight percent.

viii. The percentage of crystallinity for 0.7 PVDF + 0.3 BST is 49.92 % for 0.3 PVDF + 0.7 BST 48.29 % and for 0.5 PVDF + 0.5 BST is 53.71.

4.2 Future Scope:

The studies consisting in this dissertation, further suggests need of some studies which are very important from academic, scientific and technical point of view. They are as follows:

- The dielectric behavior of PVDF- BST nanocomposite need to be investigated. This will provide the information about dielectric relaxation and perculation threshold.
- The capacitive behavior of Metal-Insulator-Metal (M-I-M) capacitor formed by PVDF-BST nanocomposite is also of immense technological importance. This capacitor may have high breakdown strength and maderate dielectric constant, which is essential for high energy strength.

REFERENCES:

1. S. Maensiri, W. Nuansing, J. Klinkaewnarong, P. Laokul, J. Khemprasit, *Journal of Colloid and Interface Science*,,**297**,578(2006).
2. S. hua and W. fen Jiang, *Int. Journal of Minerals, Metallurgy and Material*,**19**,8(2012).
3. S. Ke, H. Huang, H. Fan, H. L. W. Chan, L. M. Zhou, Solid State Ionics, **179**, 1632(2009).
4. C. Kittel, *Introduction to Solid State Physics (John Wiley and Sons, Inc. 7th ed*. (1996)).
5. V. Tura, L. Mitoseriu, C. Papusoi, T. Osaka and M. Okuyama, *Journal of Electroceramics*, **2:3** , 163(1998).
6. S. Lahiry, V. Gupta, K. Sreenivas, and A. ManSingh, *IEEE Transactions onUltrasonic, Ferroelectrics and Frequency Control*,**47**,854(2000).
7. V. Somani, S. J. Kalita, *Journal of Electro Ceram*, **18**, 57 (2007).
8. M. Ivankovic, I. Brnardic, H. Ivankovic, M. Huskic, A. Gajovic, *Polymer*, **50**, 2544 (2009).
9. Y. C. Li, S. C. Tjong, R. k. Y. Li, *Express Polymer letters*,**5**, 526 (2011).
10. K. Verma, S. Sharma, D. K. Sharma, R. Kumar, R. Rai, *Advanced Materials Letters*, **3(1)**,44(2012).
11. C. V. Chanmal, J. P. Jog, *Express Polymer Letters*, **2**, 294 (2008).
12. H. C. Pant, M. K. Patra, A. Verma, S. R. Vadera, N. Kumar, *Acta Materialia*, **54**, 3163 (2006).
13. A. K. Tripathi, R. and P. K. C. Pillai, *Materials Letter*, **9**, 24 (1989).
14. E. Q. Huang, J. Zhao, J. W. Zha, L. Zhang, R. J. Liao and Z. M. Dang, *Journal of Applied Physics*,**115**, 194102 (2014).
15. P. Hu, Y. Song, H. Liu, Y. Shen, Y. Lin and C. W. Nan, *Journal of Materials Chemistry A*, **1**, 1688 (2013).
16. P. Barber, S. Balasubramanian, Y. Anguchamy, S. Gong, A. Wibowo, H. Gao, H. J. Ploehn and H. C. ZurLoye, *Materials*, **2**, 1697 (2009).

17. F. Stemme, M. Bruns, H. Gebwein, M. S. Zegar, M. D. Drahus, R. A. Eichel, F. Paul, J. Haubelt, J. Haubelt, J. R. Binder, *Journal of Material Science*, **47**, 6929 (2012).
18. B. Schumacher, H. Gebwein, J. Haubelt, T. Hanemann, *Microelectronic Engineering*, **87**, 1978 (2010).
19. B. H. fan, J. Weizha, D. Wang, J. Zhao, and Z. M. Dang, *Applied Physics Letters*,**100**, 012903 (2012).
20. Christopher W. Beier, Jason M. Sanders, and Richard L. Brutchey, *Journal of Physical Chemistry C*, **117**, 6958 (2013).
21. S. Gross, D. Camozzo, V. D. Noto, L. Armelao, E. Tondello, *European Polymer Jounal*,**43**, 673 (2007).
22. A. W. M. de Laat, W. P. T. Derks, *Colloids and Surfaces*, **71**, 147 (1993).